Size-Dependent Hydrogenation Selectivity of Nitrate on Pd−Cu/TiO_2 Catalysts

Fuxiang Zhang, Shuang Miao, Yali Yang, Xiu Zhang, Jixin Chen, and Naijia Guan*

Lab of Functional Polymer Materials, N & T Joint Academy and Department of Materials Chemistry, College of Chemistry, Nankai University, Tianjin, 300071, People's Republic of China

Received: January 4, 2008; Revised Manuscript Received: February 27, 2008

Catalytic hydrogenation of nitrate (NO_3^-) in water on Pd−Cu ensembles has been denoted as a promising denitridation method, but its hydrogenation selectivity remains challenging. In this study, the hydrogenation selectivity of nitrate on the Pd−Cu/TiO_2 systems was discussed mainly concerning the size effect of Pd−Cu ensembles in a gas−liquid cocurrent flow system. Demonstrated by their TEM images, homogeneous morphologies as well as narrow size distributions of Pd−Cu ensembles on titania have been prepared by a facile photodeposition process, and the size of the ensembles was controlled and varied with the total metal loadings. The different XRD patterns and XPS spectra of Pd−Cu/TiO_2 catalysts from their corresponding monometallic counterparts suggested the formation of Pd−Cu complex on the surface of TiO_2. It is first indicated that the hydrogenation selectivity of nitrate generally depends on the size of active phase with critical size of approximately 3.5 nm, below which NO_2^- becomes the predominant product instead of nitrogen. Ammonium production was increasing slowly throughout the reaction, but this can be efficiently restrained by bubbling CO_2. The optimal catalytic activity and nitrogen selectivity of 99.9% and 98.3% respectively could be achieved on the Pd−Cu/TiO_2 catalyst with average size of 4.22 nm under the modification of CO_2 after approximately 30 min reduction. The catalytic activities of nitrite on several Pd−Cu bimetallic catalysts were examined to strongly depend on the size of active metal, as is well responsible for the observed distinct hydrogenation selectivity of nitrate.

1. Introduction

Highly concentrated nitrate and its corresponding metabolites are toxic for human health and particularly harmful to infants, so the World Health Organization (WHO) recommends a maximum nitrate concentration of 10 mgN/L (calculated by nitrogen weight, denoted as mgN/L), nitrite of 0.03 mgN/L and ammonium of 0.4 mgN/L, in drinking water. However, nitrate in the groundwater of some regions is as high as 50 mgN/L. Biological and physicochemical treatment has been developed to deal with excess nitrate, but catalytic denitridation as an emerging technology has attracted intensive attention because of its more economical and ecological merits.[1–3]

Since 1989, when a Pd−Cu bimetal catalyst was found to be active by Tacke and Vorlop,[4,5] the activity and selectivity of nitrate hydrogenation on Pd−Cu bimetallic catalysts have been extensively discussed and found to be related to the structure of active components and the properties of supports.[6–27] Various supports such as Al_2O_3,[6,7,11,14,17] clay,[9] active carbon,[18,19,22,23,26] beta-zeolite,[20,21] ZrO_2,[10] SnO_2,[15] Pumice,[11] glass fiber,[12] resins,[13,25] hydrotalcite,[8,16] TiO_2,[27] and mordenite[24] have been examined.

As for the nitrate hydrogenation on the Pd−Cu catalysts, the generally accepted mechanism can be described in Figure 1,[4,5,11,18,27,32] where the catalytic hydrogenation of nitrate was considered to only take place over metal ensembles composed of Pd and Cu atoms, while nitrites as intermediates can be reduced on the surface of palladium. It was reported that the catalytic hydrogenation of nitrate does not occur without the involvement of the Pd/Cu ensemble, while nitrite as well as other consequent intermediates can be further reduced on the surface of palladium. Recently, the hydrogenation of nitrate on monometallic palladium or platinum catalysts was also demonstrated to proceed by means of the promoting effect of the metal oxide supports such as TiO_2, CeO_2, or SnO_2,[28–31] but the monometallic catalysts with satisfying activity, nitrogen selectivity, and stability have not achieved. The Pd−Cu catalysts are still considered to be the most promising for this process.

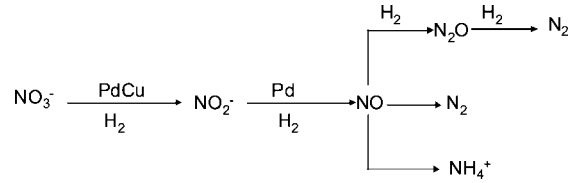

Figure 1. Hypothetical reaction scheme for catalytic hydrogenation of nitrate on Pd−Cu catalysts.

To date, many factors including support, metal composition, preparative method, and operation conditions have been discussed to provide insight into the catalytic selectivity.[2,9,11,12,15,23–27,33–36] It was suggested[36,37] that using formic acid instead of hydrogen as a reducing agent can improve the selectivity to nitrogen owing to the in situ buffering effect of formic acid that lowers the pH gradient. CO_2 bubbling played the same role in suppressing the rapid growth of the pH value.[2,7,9,11,12,15,27] A competitive adsorption from coexist ions (SO_4^{2-}, CO_3^{2-}, HCO_3^-, etc.) on Pd−Cu active sites led to the decrease of catalytic activity and selectivity of nitrate.[11,27] Unfortunately, the bimetallic catalysts with satisfying nitrogen selectivity and activity remains challenging, and more fundamental work should be carried out for further insights.

The dependence of catalytic performance on the size of active phase is commonly found in most catalytic processes. However, to the best of our knowledge, the size effect of Pd−Cu ensembles on the selectivity of nitrate hydrogenation remains

* Corresponding author. Phone/Fax: +86-22-23500341. E-mail: guannj@nankai.edu.cn.

10.1021/jp800060g CCC: $40.75
Published on Web 04/24/2008

unknown. In this study, a series of Pd−Cu/TiO_2 catalysts with different composition and size of Pd−Cu ensembles were prepared via a facile photodeposition route and used for the hydrogenation of nitrate in water. Dissimilar catalytic selectivity on them were first demonstrated and found to be related to the size of active phase. Meanwhile, transmission electron microscopy (TEM), X-ray diffraction (XRD), X-ray photoelectron spectroscopy (XPS), and atomic absorption spectrometry (AAS) were employed for the characterizations of structure.

2. Experimental Section

2.1. Catalyst Preparation and Characterization. All materials and solvents are of analytical grade and used without further purification. The water used is doubly distilled. TiO_2 is nonporous Degussa P-25, (mainly anatase, with a surface area of ca. 50 $m^2 \cdot g^{-1}$). First of all, monometallic Pd/TiO_2 catalysts with different palladium contents were prepared by a pH-controlled photodeposition method reported in our previous work.[39] Subsequently, to an aqueous solution (160 mL) of $CuAc_2 \cdot 3H_2O$ (calculated according to the copper content), the as-prepared Pd/TiO_2 (500 mg) and ethanol (4 mL) were added, and the pH value of obtained slurries was adjusted and maintained at the region of 12∼12.5 that was monitored at 10 min intervals during irradiation. After 3 h UV irradiation with 250 W high-pressure mercury lamp (the UV intensity: ca. 4 mw/cm^2), the catalyst powder was filtered, washed, and dried in air. The as-prepared Pd−Cu/TiO_2 catalysts were denoted as Cat A, Cat B, Cat C, and so forth and characterized by atom absorption spectroscopy (AAS), TEM, XRD, and XPS. For comparison, the monometallic Cu/TiO_2 and Pd/TiO_2 catalysts were prepared in the same way.

Transmission electron microscopy (TEM) was carried out on a Philips EM-120 TEM instrument with accelerating voltage of 100 KeV. The particles obtained after the irradiation and workup were dropped onto the surface of a carbon membrane supported on a copper grid and dried under ambient conditions before analysis. X-ray diffraction (XRD) patterns were collected on a D/max-2500 commercial instrument (Cu Kα, $\lambda = 1.54178$ Å) with a scan speed of $2\theta = 8.0$ deg/min. X-ray photoelectron spectroscopy (XPS) was performed using a PHI 5300 ESCA commercial instrument (PHI Inc.; Mg Kα radiation; 1253.6 eV; 10^{-7} Pa) using C 1s photoelectron peak (binding energy at 284.6 eV) as the energy reference. Atomic absorption spectrometry (AAS) was performed using an HTAZHI 180−80 (Japan).

2.2. Catalytic Tests. The catalytic reduction of nitrate and/or nitrite was performed in a 100 mL pyrex glass reactor, equipped with an electromagnetic stirrer and temperature control unit. The simplified schematic diagram of the experimental setup was presented previously.[27] The gas flow rate of 150 mL/min was well above the hydrogen-limited conditions, ensuring independence of activity and selectivity from hydrogen limitation. Before the catalytic runs, the catalysts were purged with nitrogen and then with hydrogen to remove adsorbed oxygen. The mixture was violently stirred to eliminate problems of gas diffusion. The extent of reaction was monitored by periodically withdrawing samples to analyze the concentration of nitrate, nitrite, and ammonium ions in the supernatant after centrifugation. The general reaction conditions, listed in Table 1, were used in this work unless otherwise stated, from which it can be calculated to have the total formation of nitrogen as approximately 3.57×10^{-4} mol. The temperature of the reaction mixture was set at 303 K, controlled within ±0.1 K. The initial pH value of the aqueous solution, determined with a digital pH meter (TOLEDO 320-S), was adjusted at approximately 6.0.

TABLE 1: Operating Conditions

temperature	303 K
initial pH value	6.0
total pressure	1 bar
hydrogen partial pressure	1 bar
reaction volume	100 mL
catalyst weight	0.1 g
initial nitrate concentration in the reactor[a]	100 mgN/L
nitrate source	KNO_3
nitrite source	$NaNO_2$
gas flow rate	150 mL/min
reaction time	10 min

[a] Calculated by nitrogen weight (mgN/L), and the same to NO_2^- and NH_4^+. The same hereinafter.

Doubly distilled water was the reaction medium for the nitrate and nitrite reductions. The concentration of palladium and copper ions in the solution after reaction was measured by AAS. With the detection limitation of AAS, no metal ions were observed, indicating good chemical stability of the as-prepared Pd−Cu/TiO_2 catalysts.

The concentrations of nitrate, nitrite, and ammonium ions in the aqueous solution were determined by colormetric method with an UV−vis spectrophotometer (Shimadzu, UV-240); the detailed procedures are described elsewhere.[27] Generally, nitrate, nitrite, and ammonium ions were colored by a dyeing agent and then measured their absorption intensity at 410 nm, 540 nm and 697 nm separately. All of the concentrations were normalized by nitrogen weight (mgN/L). The gas product was analyzed with a gas chromatograph (GC) equipped with molecular sieves 5 A (for N_2 and O_2) and Porapak Q (for N_2O) columns. It should be mentioned that, for all of the experiments, no N_2O was detected, so the selectivity of N_2O will not be discussed in the study.

3. Results

3.1. Characterizations of Catalysts. All of the catalysts were characterized by TEM, AAS, XRD, and XPS to study their morphology and surface structure. The AAS analysis indicated that the deposition efficiency of metal by the photodeposition method on every catalyst is approximate to 100%. As indicated in Table 2, the total metal content and metal ratio of the as-prepared Pd−Cu/TiO_2 catalysts in this study varied from 1 wt% to 20 wt% for metal content and from 1:1 to 5:1 for the ratio of Pd:Cu, respectively. As far as the catalysts denoted as Cat A−E with total metal content of 1 wt% are concerned, the size of active phase was slightly changed with the variation of Pd:Cu ratio, and all of which are approximate to 1.7 nm. Nevertheless, as for the samples (Cat D, H, I, J, and K) with Pd:Cu ratio of 4:1 but different total metal content, the average size of Pd−Cu assembles obviously increased from approximately 1.7 to 4.2 nm when the total metal content varied from 1 wt% to 20 wt%. All of the size data of deposited metal are statistically averaged and calculated from their corresponding TEM images.

The morphology and size of deposited metals on titanium dioxide were investigated by TEM, and typical images of Cat D (1 wt%), H (3 wt%), and K (20 wt%) are given in Figure 2. The homogeneous morphologies of deposited metals are all the view in this study. The corresponding histograms of metal size distribution shown in Figure 2d−f demonstrate the narrow size distribution very well, whose average metal sizes are measured as 1.75, 1.84, and 4.22 nm for Cat D, Cat H, and Cat K respectively. It indicates that, using the soft photodeposition

TABLE 2: Composition of Active Phase As Well As Their Hydrogenation Performance on the As-Prepared Pd−Cu/TiO_2 Catalysts

	active composition				catalytic performance			
	content (%)					concentration (mgN/L)		
catalyst	total/Pd:Cu	Pd	Cu	size (nm)	nitrate conversed (mgN/L)	NO_2^-	NH_4^+	N_2
Cat A	1.03 /1:1	0.52	0.51	1.68	30.2	21.4	3.4	5.4
Cat B	0.99 /2:1	0.67	0.32	1.67	67.9	43.5	5.0	19.4
Cat C	1.01 /3:1	0.77	0.24	1.71	77.0	43.6	5.3	28.1
Cat D	1.02 /4:1	0.81	0.21	1.75	88.9	43.5	5.6	39.8
Cat E	1.01 /5:1	0.84	0.17	1.72	84.4	44.3	5.7	34.4
Cat F	2.02	2.02	0	1.76				
Cat G	1.99	0	1.99	1.78				
Cat H	3.05 /4:1	2.43	0.62	1.84	81.8	44.3	5.9	31.7
Cat I[a]	12.07 /4:1	9.65	2.42	3.06	99.5	43.6	6.0	49.9
Cat J[a]	14.99 /4:1	12.04	2.95	3.51	99.4	0.7	6.8	91.9
Cat K[a]	19.98 /4:1	15.96	4.02	4.22	99.5	0.2	7.3	92.0

[a] Reaction time: 30 min.

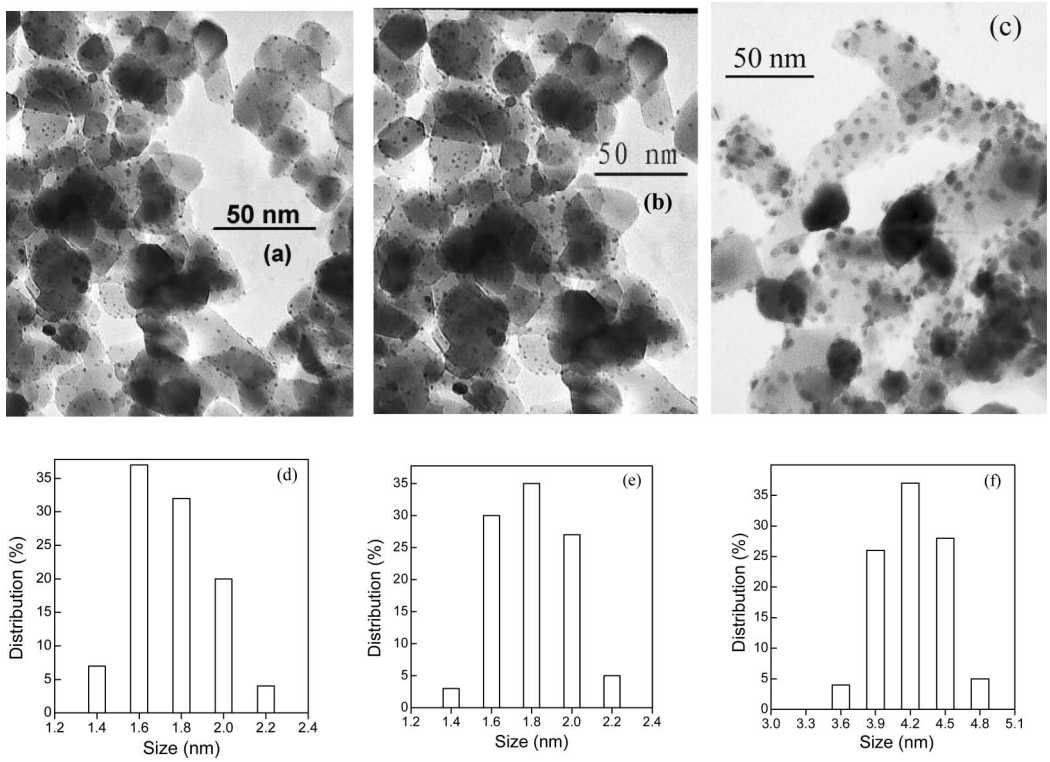

Figure 2. Typical TEM images of Pd−Cu/TiO_2 catalysts (a) Cat D, (b) Cat H, and (c) Cat K, and the size distribution histogram of catalysts (d) Cat D, (e) Cat H, and (f) Cat K.

process, the size of the deposited bimetallic Pd−Cu ensembles can be well-adjusted by the variation of metal precursor concentration. The preparative principles can be referred to in our previous work.[39]

The crystalline phase and state of deposited metals on the as-prepared Pd−Cu/TiO_2 composites were analyzed by XRD measurements. Figure 3 showed the representative XRD patterns of Cat J (Pd−Cu/TiO_2, 15 wt%, Pd:Cu = 4:1), Pd/TiO_2 (12 wt%), and pure TiO_2 powder. According to Scherrer's equation, the average size of deposited palladium on Pd/TiO2 (12 wt%) was calculated as approximately 3.3 nm. Consistent with the corresponding monometallic counterparts, no characteristic peaks of palladium or copper species were detected on the bimetallic catalysts with a total metal <6 wt% (not given), suggesting homogeneous dispersion of the metals deposited on titania. Comparatively, the observed three more peaks at 2θ = 40.06°, 46.5°, and 82.6° on 12 wt% Pd/TiO_2 particles than those on parent TiO_2 can be ascribed to the (111), (200), and (311) diffraction peaks of metallic palladium. However, the characteristic peaks of metallic palladium disappear on the sample Cat J (Pd−Cu/TiO2, 15 wt%, Pd:Cu = 4:1), and no obvious new diffraction peaks are observed. It means that the deposition of copper has changed the structure and crystalline phase of palladium on the Pd/TiO_2 sample. Alternatively, copper may have incorporated into the framework of palladium particles to produce Cu−Pd ensembles. Because of the use of soft preparative route free of calcinations, the crystalline phase and size of the support TiO_2 were well-maintained in this study.

To provide further insight into the different structure properties between the Pd−Cu/TiO_2 composite and its monometallic counterparts, their XPS spectra were examined. Meanwhile, the XPS spectra of bimetallic catalysts before and after reactions

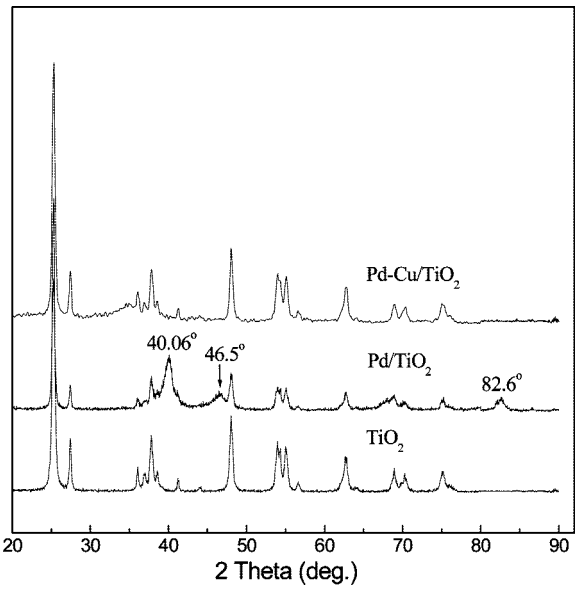

Figure 3. Representative XRD patterns of Pd−Cu/TiO_2 (Cat J, 15 wt%; Pd:Cu = 4:1) and Pd/TiO_2 (12 wt%) catalysts.

TABLE 3: Valence States of Metals Deposited on Bimetallic and Monometallic Catalysts

catalyst	major species for Pd		major species for Cu	
Pd−Cu/TiO_2	before reaction	after reaction	before reaction	after reaction
	Pd + PdO_2	Pd + PdO	Cu	Cu + Cu_xO
Pd/TiO_2	Pd			
Cu/TiO_2			Cu_xO, Cu	

were also investigated to discuss the exact active phase for nitrate hydrogenation (see Supporting Information). On the basis of their binding energies, all of the spectra were assigned and summarized in Table 3. As for the bimetallic catalysts before and after reaction, three different valence states of Pd, PdO, and PdO_2 with binding energies of approximately 335.1 (or 334.8), 336.5, and 337.6 eV, and two different valence states of Cu and Cu_xO (binding energies of ca. 932.5/931.9 and 934.4 eV) are primarily observed. The change in valence states of Pd and Cu before and after reaction indicates their participation in the hydrogenation process of nitrate. It is also different from their monometallic counterparts, on which Pd and PdO species with binding energy of 335.7 and 336.8 eV and Cu and Cu_xO with binding energy of 932.5 eV and 934.7 eV are mainly observed. The discrepancy in valence states of monometallic and bimetallic catalysts demonstrates the changes of palladium species and formation of a new phase composed of palladium and copper on the bimetallic catalysts, in accordance with the XRD results obtained.

3.2. Catalytic Performances. As shown in Table 2, the hydrogenation performances of nitrate on the as-prepared bimetallic catalysts are greatly influenced by the composition and size of active metals deposited on titania. The hydrogenation activities can be classified into two cases with the boundary on Cat J whose average active phase size is 3.51 nm. For the catalysts (Cat A−I) with average metal size below 3.5 nm, a great amount of nitrite ions was formed and most of which have the concentration of 43−44 mgN/L. On the other two catalysts Cat J and K with metal size of 3.51 and 4.22 nm, respectively, the residual nitrite ions after 30 min hydrogenation were greatly reduced to approximately 0.2 mgN/L, and the selectivity of nitrogen as a desirable product was significantly enhanced. This reveals that the hydrogenation selectivity of nitrate is greatly correlated to the size of active metals. In comparison, the catalytic performances on Cat A−E are also dependent on the composition of active phase, and the optimal weight ratio of Pd:Cu should be 4:1 in consideration of the catalytic activity. Ammonia ions as byproduct are observed to have the concentration of approximately 3−7 mgN/L on all of the catalysts tested. Concerning the monometallic Pd/TiO_2 (Cat F) and Cu/TiO_2 (Cat G) catalyst, no obvious hydrogenation of nitrate was observed similar to most results of literature. It is worthy to note that the residual nitrite ions of as high as approximately 44 mgN/L in the postreaction solution were mostly observed on the systems with a bimetallic size below 3.5 nm.

To concern the special dependence of the residual concentration of nitrite ions on the bimetallic size, the time curves of nitrate hydrogenation on the catalysts Cat E (1.72 nm) and Cat K (4.22 nm) were selectively examined and plotted in Figure 4a,b, respectively. In both cases, the concentration of nitrate (decreasing) and ammonium (increasing) are as expected, but the catalytic behaviors of nitrite ions on them are typically dissimilar. On the Cat E (Figure 4a), the concentration of nitrite rapidly increases to a steady level of approximately 44 mg•L^{-1} after 5 min reduction, different from previous literatures,[15,27] while on Cat K (Figure 4b), the concentration of nitrite first undergoes an increase and subsequent decrease. Since the reaction time on Cat E was prolonged to 60 min, the possibility of nitrite further self-catalysis can be ruled out from the fact shown in Figure 4a that the concentration of initial nitrite ions was almost constant until the depletion of nitrate. Accordingly, a reasonable explanation to the residue of highly concentrated nitrite is that catalytic reduction of nitrite on the catalysts with the size of active phase below 3.5 nm does not happen or proceeds at an extremely low rate.

To actually know about the catalytic behavior of nitrite, the best way should be the investigation on the direct hydrogenation of nitrite on several typical catalysts, which were carried out with an initial nitrite concentration of 45 mgN/L (close to the steady level of 43−44 mgN/L). As shown in Table 4, only 1.2% and 1.4% were conversed on the catalysts Cat E and Cat I with bimetallic size of below 3.5 nm respectively after 10 min reduction. Comparatively, conversions of higher than 99% on Cat J and Cat K with the size of metals higher than 3.5 nm were achieved. It indicates that the hydrogenation of nitrite strongly depends on the size of active phase. Accordingly, it is reasonable to deduce that the residue of high concentrated NO_2^- on the catalysts with the size of active sites below 3.5 nm should be ascribed to the extremely low hydrogenation rate of nitrite. Conversely, on the catalysts of Cat J and Cat K with the metal size above 3.5 nm, the nitrite ions produced from nitrate can be further reduced so that the accumulation of nitrite ions will then avoided.

It is noteworthy that the selectivity of nitrite hydrogenation on these catalysts is also different (Table 4). On the catalysts Cat E and Cat I, nitrite was mostly reduced into ammonium ions, while nitrogen is the main product on the Cat J and Cat K (Table 4). Furthermore, the hydrogenation selectivity of nitrite on the catalysts Cat E and Cat I are also dissimilar to that of nitrate hydrogenation (see Table 2) in which a great amount of nitrogen instead of ammonium was formed. To comment on this point, the course of nitrate hydrogenation on Cat E in 10 min was monitored to understand the reaction essence. It is demonstrated (Table 1 in Supporting Information) that the reduction behaviors of nitrate before and after 4 min are obviously different: one is to form mainly nitrite ions in the

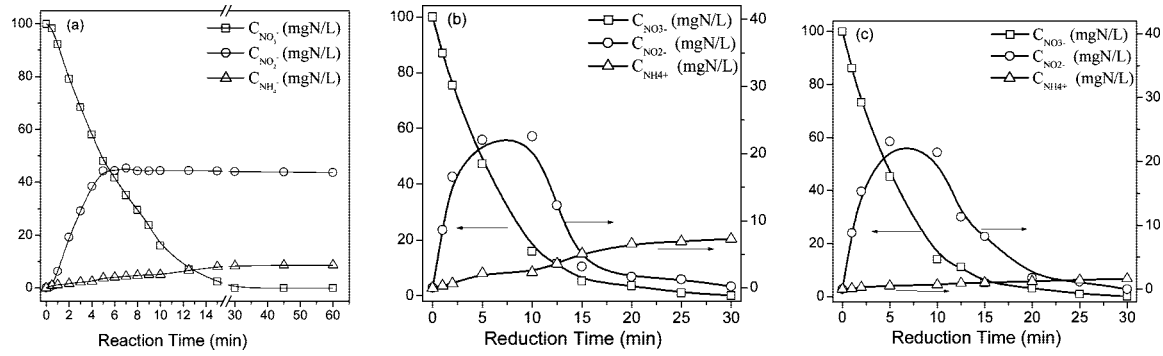

Figure 4. Time curve of nitrate hydrogenation on the catalysts Cat E and Cat K: (a) Cat E, (b) Cat K, and (c) Cat K with CO_2 bubbling. Average size of active phase: Cat E of 1.72 nm, Cat K of 4.22 nm.

TABLE 4: Hydrogenation of Nitrite on the Pd−Cu/TiO_2 Catalysts with Different Size of Active Phase (Reaction Time = 10 min, Initial Concentration: 45 mgN/L)

catalyst	size of metals (nm)	conversion (%)/ Conversed NO_2^- (mgN/L)	NH_4^+ produced (mgN/L)	selectivity/N_2 produced (mgN/L)
Cat E	1.72	1.2/0.5	0.5	
Cat I	3.06	1.4/0.6	0.6	
Cat J	3.51	99.4/44.8	2.0	95.6/42.8
Cat K	4.22	99.8/44.9	1.7	96.2/43.2

early stage of nitrate hydrogenation, and the other produces nitrogen in the later stages. In the initial 3 min, the amount of nitrate reduced matches the sum of nitrite and ammonium ions produced, demonstrating the high selectivity to these two products. Subsequently, the concentration of NO_2^- remains constant, and nitrogen becomes the predominant product. Ammonium is slowly formed as a byproduct throughout the reaction.

Similar to most previous observations,[2,7,27] pH value of the reaction solution was increased with continuous formation of OH^- during the hydrogenation of nitrate. To inhibit the overproduct of ammonium, CO_2 was bubbled as an attempt during the hydrogenation of nitrate on the catalyst Cat K with average size of 4.22 nm. As shown in Figure 4c, the decay curves of nitrate and nitrite as intermediate species are similar to that on Cat K without CO_2 bubbling (Figure 4b), but the amount of ammonium produced is greatly reduced. The hydrogenation of nitrate primarily conducts toward the formation of nitrogen. After 30 min hydrogenation, the residual concentration of nitrate and nitrite was decreased to 0.1 and 0.01 mgN/L respectively, and the activity and nitrogen selectivity were calculated as 99.9% and 98.3% respectively.

4. Discussion

The hydrogenation of nitrate on Pd−Cu catalysts has been proposed to have nitrite intermediates.[11,18,32] The Cu−Pd ensembles deposited on the supports can provoke the hydrogenation of nitrate to nitrite at the first step; subsequently, hydrogenations of nitrite to nitrogen and ammonia (the second step) proceed only on Pd aggregates on the Cu−Pd catalysts.[18] The hydrogenation of nitrite as a critical step becomes therefore important in the selectivity of N_2 and NH_4^+.[6,11,18,19]

It was suggested[36] that the formation mechanisms of nitrogen and ammonium are dissimilar because the formation of nitrogen containing two nitrogen atoms requires a pairing of two nitrogen-containing surface species (N species) originating from the substrates nitrate or nitrite produced. However, the formation of ammonium commonly results from the meeting of N species and reductant species covered on the surface of active sites by a diffusion effect. Therefore, the selectivity was suggested as a function of the ratio of surface coverage of N species to reductant species (N:reductant ratio).[36,38] The higher the N:reductant ratio is, the higher the nitrogen selectivity will be. Similarly, increasing exposed surface of active metals will create more opportunities to simultaneously absorb two N species for the formation of nitrogen. Hence, the size of active sites should be another parameter for influencing the hydrogenation selectivity. Since the hydrogenation of nitrite can produce commonly on the monometallic palladium sites, the selectivity of nitrate hydrogenation will be determined by the size of palladium particles as well as the N:reductant ratio on the palladium sites.

It is reasonable to deduce that a moderate amount of bimetallic ensembles and suitable size of palladium ensembles are desirable for the activity and selectivity of nitrate hydrogenation respectively. Commonly, catalysts with different ratios and contents of bimetals have distinct surface compositions and size of palladium ensembles, respectively. A higher ratio of Pd:Cu can be expected to form fewer bimetallic ensembles but more monometallic palladium ones. As far as the catalysts of Cat A−E with the same total metal weight of 1 wt% are concerned, the optimal ratio of Pd:Cu in this study can be judged as 4:1 (Cat D) from the fact that the hydrogenation activity of nitrate on Cat D was optimal. In this study, both XRD patterns and XPS spectra have indicated the formation of Pd−Cu ensembles and the lack of single palladium particles from the disappearance of diffraction peaks assigned to metallic palladium. However, some palladium uncombined with copper (exposed palladium) can be expected to exist from the demonstration of XPS spectra on Pd−Cu/TiO_2 catalysts where metallic palladium as well as PdO_2 was also observed (see Table 3). The exposed palladium should be the active sites for nitrite reduction. It means that the individual palladium particles do not exist on the bimetallic catalysts, but there exist some exposed palladium surface on the Pd−Cu ensembles, as can be responsible for the hydrogenation of nitrite intermediates.

It is difficult to determine the exact size of pallaium on the Pd−Cu ensembles, but it is reasonable to deduce that, as for the catalysts with the same ratio of Pd:Cu, the smaller the size of Pd−Cu ensembles is, the smaller the size of exposed palladium particles will be. On the other hand, the exposed palladium species are not interconnected with each other because of the existence of copper interface. Accordingly, the difficulty in the simultaneous absorption and activation of two N species becomes distinct on these active sites. On the basis of our experimental results, it can be suggested that, on the bimetallic ensembles with size of below 3.5 nm, the exposed palladium particle becomes too small to adsorb and activate two N species

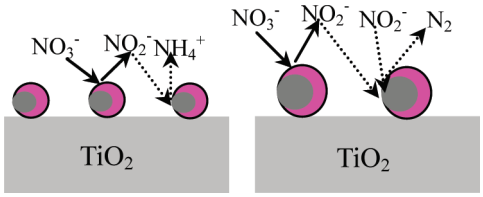

Figure 5. Selective hydrogenation mechanism of nitrate on the Pd−Cu/TiO_2 catalysts with different size of active phase: (left) < 3.5 nm; (right) > 3.5 nm. (●:Pd−Cu ensembles. ●:exposed palladium sites).

simultaneously for the formation of nitrogen. Oppositely, the hydrogenation of nitrite produced from nitrate will proceed. Since the formation of ammonium required only one N species, the size effect is not remarkable, and ammonium as byproduct was observed for all of the systems. Regarding the phenomena that the selectivity of nitrogen was greatly improved in the late stage of nitrate hydrogenation on Cat E, it may result from the fact that the increasing nitrite produced from nitrate reduction will enhance the N:reductant ratio on the palladium sites and provide the exposed palladium species with more opportunities to adsorb simultaneously two N species. One proof to that is the result of nitrate hydrogenation on Cat E (1.72 nm) that, when 45 mgN/L nitrite was added into the initial solution containing 100 mgN/L nitrate to improve the N:reductant ratio, the selectivity of nitrogen was exactly enhanced reaching 90%.

Generally, an increase of pH value in most nitrate hydrogenation was observed because of the production of OH^-, and ammonia formation was found favorable at higher pH values.[2,7,27] Similarly, the pH value was measured increasing and a great amount of side-product ammonium was formed in this study. It has been suggested that the acid sites present on the surface of some supports may act as the neutralization agent to inhibit the pH increasing by the diffusion effect in the bulk of the solution.[15] To date, however, bubbling CO_2 into the reaction solution to buffering produced hydroxyl ions is still a simple and effective approach to keeping the pH value constant. Originating from the inhibition of ammonium product after CO_2 bubbling in this study, the selectivity of nitrogen was consequently enhanced. However, the catalytic conversion of nitrate has not been improved. Thus, it can be interfered that the addition of CO_2 as an efficient pH buffering may only change the reduction path of the intermediate nitrite, but no effects happen to the course of nitrate-to-nitrite reduction.

In summary, the bimetallic Pd−Cu ensembles were commonly considered as the main active sites of nitrate to nitrite, and monometallic palladium is the main active site of nitrite hydrogenation.[4,5,11,18,32] In this study, the hydrogenation of nitrate was mainly assigned to the activation on the Pd−Cu bimetallic sites as desirable, and the reduction of nitrite was suggested to happen on the exposed palladium surface. The hydrogenation of nitrite strongly depends on the size of the exposed palladium, so the selectivity of nitrate hydrogenation is greatly correlated to the size of Pd−Cu ensembles. The size dependent selective hydrogenation mechanism of nitrate can be described as Figure 5, where nitrate is first activated on the Pd−Cu active sites to produce nitrite that was subsequently readsorbed on the exposed palladium sites for the formation of ammonium or nitrogen. On the surface of palladium with distinct size, the selectivity of ammonium and nitrogen is not similar.

5. Conclusion

The hydrogenation selectivity of nitrate on the Pd−Cu/TiO_2 catalysts with different total metal loadings and ratios was discussed and found to be strongly related to the size of Pd−Cu ensembles. The Pd−Cu ensembles with sizes above 3.5 nm are suitable for simultaneous absorption and activation of two N-containing species, which is responsible for the formation of nitrogen. As a matter of fact, the size-dependent hydrogenation selectivity of nitrate is mainly determined by the hydrogenation performance of nitrite as the intermediate specie which was testified to be influenced by the size of exposed palladium on the Pd−Cu ensembles. Ammonium as a byproduct all along can be efficiently inhibited by the pH buffering effect of CO_2 bubbled. The maximum catalytic activity and nitrogen selectivity of above 99% and 98.3% was achieved in this system after approximately 30 min hydrogenation. This research also demonstrates that the hydrogenation performance of nitrite should be paid more attention, as it provides insight into the hydrogenation selectivity of nitrate.

Acknowledgment. The authors are grateful for the financial support of National Basic Research Program of China with Grant 2003CB615801 (also called 973), NSFC with Grants 20233030, 20573059, 20603019, and 20777039, and Fok Ying Tung Education Foundation. The authors thank China National Academy of Nanotechnology & Engineering for some measurements.

Supporting Information Available: XPS spectra of bimetallic Pd−Cu/TiO_2 catalyst before and after reaction and the XPS spectra of the corresponding single catalysts Pd/TiO_2 and Cu/TiO_2 are given. The detailed data of nitrate hydrogenation on Cat E are provided. This material is available free of charge via the Internet at http://pubs.acs.org.

References and Notes

(1) Matatov-Meytal, U. I. *Ind. Eng. Chem. Res.* **2005**, *44*, 9575.
(2) Pintar, A.; Setinc, M.; Levec, J. *J. Catal.* **1998**, *174*, 72.
(3) A, E.; Palomares, J. G.; Prato, F.; Rey, A. Corma. *J. Catal.* **2004**, *221*, 62.
(4) Tacke, T.; Vorlop, K. D. *Dechema Biotechnology Conferences*; *3*, 1989, 1007.
(5) Vorlop, K. D.; Tacke, T. *Chem.-Ing.-Tech.* **1989**, *61*, 836.
(6) Ilinitch, O. M.; Cuperus, F. P.; Nosova, L. V.; Gribov, E. N. *Catal. Today* **2000**, *56*, 137.
(7) Pintar, A.; Batista, J.; Levec, J.; Kajiuchi, T. *Appl. Catal. B: Environ.* **1996**, *11*, 81.
(8) Wang, Y.; Qu, J. H.; Liu, H. J. *J. Mol. Catal. A: Chem.* **2007**, *272*, 31.
(9) Rao, G. R.; Mishra, B. G. *J. Porous Mater.* **2007**, *14*, 205.
(10) Strukul, G.; Gavagnin, R.; Pinna, F.; Modaferri, E.; Perathoner, S.; Centi, G.; Marella, M.; Tomaselli, M. *Catal. Today* **2000**, *55*, 139.
(11) Deganello, F.; Liotta, L. F.; Macaluso, A.; Venezia, A. M.; Deganello, G. *Appl.Catal. B: Environ.* **2000**, *24*, 265.
(12) M-Meytal, Y.; Barelko, V.; Yuranov, I.; Kiwi-Minsker, L.; Renken, A.; Sheintuch, M. *Appl. Catal. B: Environ.* **2001**, *31*, 233.
(13) Pintar, A.; Batista, J.; Levec, J. *Chem. Eng. Sci.* **2001**, *56*, 1551.
(14) Daub, K.; Wunder, V. K.; Dittmeyer, R. *Catal. Today* **2001**, *67*, 257.
(15) Gavagnin, R.; Biasetto, L.; Pinna, F.; Strukul, G. *Appl. Catal. B: Environ.* **2002**, *38*, 91.
(16) Palomares, A. E.; Prato, J. G.; Marquez, F.; Corma, A. *Appl. Catal. B: Environ.* **2003**, *41*, 3.
(17) Pintar, A.; Batista, J.; Muševič, I. *Appl. Catal. B: Environ.* **2004**, *52*, 49.
(18) Yoshinaga, Y.; Akita, T.; Mikami, I.; Okuhara, T. *J. Catal.* **2002**, *207*, 37.
(19) Mikami, I.; Sakamoto, Y.; Yoshinaga, Y.; Okuhara, T. *Appl. Catal. B: Environ.* **2003**, *44*, 79.
(20) Sakamoto, Y.; Nakamura, K.; Kushibiki, R.; Kamiya, Y.; Okuhara, T. *Chem. Lett.* **2005**, *34*, 1510.
(21) Nakamura, K.; Yoshida, Y.; Mikami, I.; Okuhara, T. *Chem. Lett.* **2005**, *34*, 678.
(22) Matatov-Meytal, U.; Sheintuch, M. *Catal. Today* **2005**, *102−103*, 121.
(23) Sakamoto, Y.; Kamiya, Y.; Okuhara, T. *J. Mol. Catal. A: Chem.* **2006**, *250*, 80.

(24) Nakamura, K.; Yoshida, Y.; Mikami, I.; Okuhara, T. *Appl. Catal. B: Environ.* **2006**, *65*, 31.
(25) Gašparovičová, D.; Králik, M.; Hronec, M.; Biffis, A.; Zecca, M.; Corain, B. *J. Mol. Catal. A: Chem.* **2006**, *244*, 258.
(26) Barrabés, N.; Just, J.; Dafinov, A.; Medina, F.; Fierro, J. L. G.; Sueiras, J. E.; Salagre, P.; Cesteros, Y. *Appl. Catal. B: Environ.* **2006**, *62*, 77.
(27) Gao, W.; Guan, N.; Chen, J.; Guan, X.; Jin, R.; Zeng, H.; Liu, Z.; Zhang, F. *Appl. Catal. B: Environ.* **2003**, *46*, 341.
(28) Epron, F.; Gauthard, F.; Barbier, J. *J. Catal.* **2002**, *206*, 363.
(29) Sá, J.; Berger, T.; Fottinger, K.; Riss, A.; Anderson, J. A.; Vinek, H. *J. Catal.* **2005**, *234*, 282.
(30) D'Arino, M.; Pinna, F.; Strukul, G. *Appl. Catal. B:Environ.* **2004**, *53*, 161.
(31) Corma, A.; Palomares, A. E.; Rey, F.; Prato, J.; G., *J. Catal.* **2004**, *227*, 561.
(32) Wärnå, J.; Turunen, I.; Salmi, T.; Maunula, T. *Chem. Eng. Sci.* **1994**, *49*, 5763.
(33) Epron, F.; Gauthard, F.; Pineda, C.; Barbier, J. *J. Catal.* **2001**, *198*, 309.
(34) Prüsse, U.; Hörold, S.; Vorlop, K.D. *Chem.-Ing.-Tech.* **1997**, *69*, 93.
(35) Berndt, H.; Mönnich, I.; Lücke, B.; Menzel, M. *Appl. Catal.B: Environ.* **2001**, *30*, 111.
(36) Prüsse, U.; Vorlop, K. D. *J. Mol. Catal. A* **2001**, *173*, 313.
(37) Prüsse, U.; Hörold, S.; Vorlop, K. D. *Chem.-Ing.-Tech.* **1997**, *69*, 87.
(38) Tacke, T. Ph.D. Thesis, TU Braunschweig, Germany, 1991.
(39) Zhang, F.; Chen, J.; Zhang, X.; Gao, W.; Jin, R.; Guan, N. *Catal. Today* **2004**, *93*−*95*, 645.

JP800060G